

# Capacitance-voltage characteristics of alternating-current thin-film electroluminescent devices

R. C. McArthur, J. D. Davidson, and J. F. Wager

Department of Electrical and Computer Engineering, Center for Advanced Materials Research, Oregon State University, Corvallis, Oregon 97331

I. Khormaee and C. N. King

Planar Systems, Inc., Beaverton, Oregon 97006

(Received 5 October 1989; accepted for publication 26 February 1990)

The capacitance-voltage ( $C$ - $V$ ) technique is proposed as a method for characterization of the electrical properties of alternating-current thin-film electroluminescent (ACTFEL) display devices. Analysis of the  $C$ - $V$  and aging characteristics of ZnS:Mn ACTFEL devices indicates that the  $C$ - $V$  technique is complementary to the charge-voltage technique in the extraction of device physics information.

The standard technique used to characterize the electrical properties of alternating-current thin-film electroluminescent (ACTFEL) display devices is charge-voltage ( $Q$ - $V$ ) analysis.<sup>1-8</sup> The purpose of this letter is to propose a complementary approach for electrical characterization of ACTFEL devices, the capacitance-voltage ( $C$ - $V$ ) technique. Since capacitance is simply the derivative of charge with respect to voltage, the  $C$ - $V$  technique can be viewed as an extension of the  $Q$ - $V$  technique.

The  $C$ - $V$  measurement is accomplished using the circuit shown in Fig. 1. An ac waveform generator with a small duty cycle drives the ACTFEL device and a 0.5–5 k $\Omega$  series resistor. For all of the data present herein, the waveform used is generated with a Wavetek model 275 Arbitrary Waveform Generator and is a 1 kHz symmetric waveform with 5  $\mu$ s rise and fall times and a 35  $\mu$ s pulse width measured at 50% of the maximum pulse amplitude. The  $C$ - $V$  curve is obtained by recognizing that

$$C = \frac{dq}{dv_2} = \frac{dq/dt}{dv_2/dt} = \frac{i}{dv_2/dt}. \quad (1)$$

The current may be obtained as the voltage difference across a series resistor:

$$i = (v_1 - v_2)/R_s. \quad (2)$$

In Eqs. (1) and (2),  $v_1$  and  $v_2$  are voltages with respect to ground as indicated in Fig. 1 and are obtained by sampling with a Tektronix model 7854 digitizing oscilloscope. The mathematical operations defined by Eqs. (1) and (2) are accomplished with the digitizing oscilloscope and the  $C$ - $V$  curve is obtained by plotting  $C$  vs  $v_2$ . The experiment is controlled with a personal computer which is also used for data storage and further data processing, if required. The viability of this method of measuring capacitance was tested by replacing the ACTFEL device with a capacitor of known value; the known capacitance was accurately determined using the above technique.

To understand the nature of the  $C$ - $V$  measurement, first consider the ideal  $Q$ - $V$  curve of an ACTFEL device, shown in Fig. 2, operating in steady state in a light emission regime. Differentiating Fig. 2 results in the ideal  $C$ - $V$  curve illustrated in Fig. 3. The minimum capacitance is that due to the total capacitance of the ACTFEL device (i.e., a series combination of the phosphor and insulator capacitances) while

the maximum capacitance is that due exclusively to the insulators as the phosphor is conducting during the charge transfer portion of the waveform.<sup>1-8</sup> Additionally, the threshold voltage indicative of the onset of charge transfer  $V_{th}$  and the maximum applied voltage amplitude  $V_m$  are indicated in Fig. 3.

In actual measurements, the  $C$ - $V$  curve is normally acquired individually for each voltage polarity and only the first half of the driver pulse waveform is acquired. Each voltage polarity waveform is acquired individually because of the extremely small duty cycle of the driver waveform which precludes high-resolution digital acquisition of two subsequent waveforms. Only the first half of the driver pulse waveform is usually acquired since the information of most relevance is contained in this regime. The second half of the pulse is essentially due to the retrace which is manifest in Fig. 3 as the portion of the  $C$ - $V$  rectangle indicated by the dashed lines. Thus, an ideal standard  $C$ - $V$  curve would look like the right half of the curve shown in Fig. 3 with the dashed line traces absent.

A  $Q$ - $V$  curve of a ZnS:Mn ACTFEL device is shown in Fig. 4. The charge  $Q$  for this curve is obtained from an integration of the current found in Eq. (2). The slopes of the straight line fits to the  $Q$ - $V$  characteristic yield the insulator and total device capacitances, as in the ideal  $Q$ - $V$  case. The intersection of these two straight line fits defines the threshold voltage. However, note deviations from ideal linear behavior near  $V_{th}$  and  $V_m$ .

To investigate these deviations from ideality in more

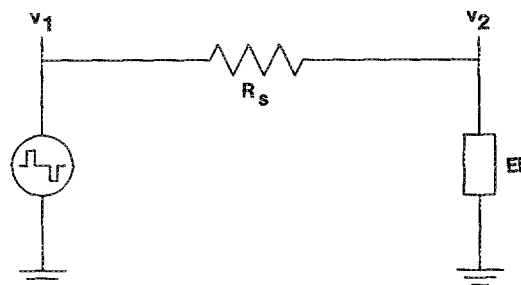


FIG. 1. Circuit used for  $C$ - $V$  analysis.

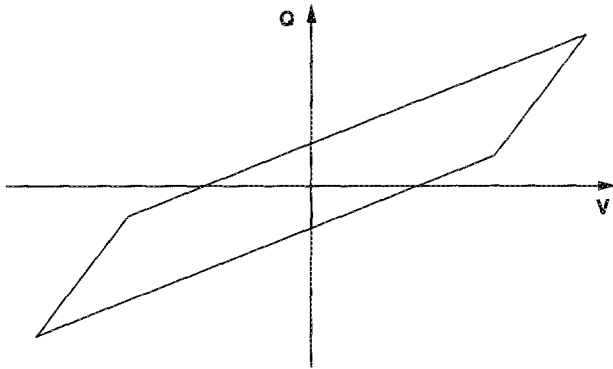


FIG. 2. Ideal  $Q$ - $V$  curve.

detail, it is convenient to focus attention on the  $C$ - $V$  curve of Fig. 5 which is derived from the same data as Fig. 4. Before Eq. (1) was used to calculate  $C$ , the numerically computed voltage derivative was filtered via least-squares approximation using piecewise, quadratic polynomials with  $B$ -spline basis functions. This operation suppresses the amplified noise due to differentiation. The horizontal portions of the  $C$ - $V$  curve are due to the constant capacitances associated with the total and insulator capacitances. The transition region near  $V_{th1}$  corresponds to the initiation of transferred charge from localized states near the interface across the ZnS, thereby exciting Mn atoms into luminescently active excited states and shunting the ZnS capacitance.

It is evident from Fig. 5 that the threshold voltage is not as clearly defined as implied by the ideal curve of Fig. 3. In fact, three different definitions of the threshold voltage from Fig. 5 are possible corresponding to the onset of the transition, the midpoint of the transition, and the saturation in which the capacitance is exclusively that of the insulator capacitance, which we denote  $V_{th1}$ ,  $V_{th2}$ , and  $V_{th3}$ , respectively. We have found that  $V_{th1}$  varies most readily with changes in the pulse width or voltage amplitude of the applied waveform while  $V_{th3}$  is relatively insensitive to these variations. We attribute  $V_{th1}$  to the onset of emission of electrons from shallow interface traps. Also, we believe that  $V_{th3}$  corresponds to the initiation of field clamping. We have also found that  $V_{th2}$  corresponds most closely to the threshold voltage found from  $Q$ - $V$  measurements.

Total and insulator capacitances calculated on the basis

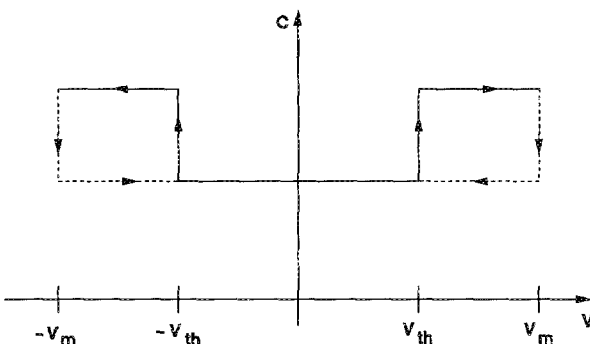


FIG. 3. Ideal  $C$ - $V$  curve obtained from differentiation of Fig. 2.

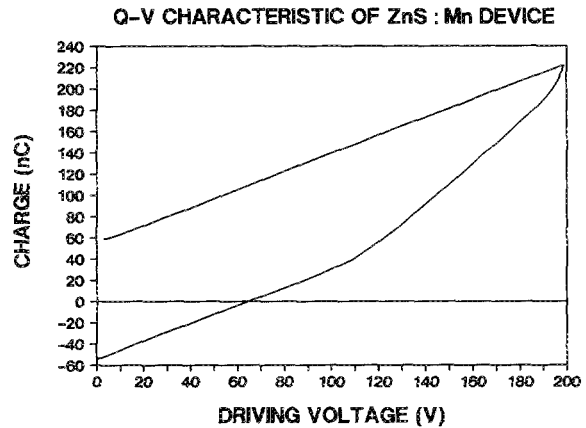


FIG. 4.  $Q$ - $V$  curve for a ZnS:Mn ACTFEL device.

of the thicknesses and dielectric constants of the insulator and phosphor layers are found to be in good agreement with values obtained from the  $C$ - $V$  measurement. It is apparent from this discussion that the  $C$ - $V$  measurement reveals more device physics information regarding the transferred charge threshold characteristics than the  $Q$ - $V$  measurement.

The second deviation from ideality which occurs in Fig. 5 is an increase in the measured capacitance at voltages near  $V_m$ . This deviation is also apparent in the  $Q$ - $V$  curve of Fig. 4. There are two possible explanations for this increase in capacitance at large applied voltages. First, the insulator leakage is large enough that the appropriate circuit model for the insulator is a resistor in parallel with the insulator capacitance such that the apparent rise in capacitance is due to a  $RC$  effect. Second, transferred charge is injected into the insulator such that the effective thickness of the insulator is reduced and the corresponding capacitance of the insulator is increased. Further work is required in order to determine which explanation is preferred.

The  $C$ - $V$  technique is useful for aging analysis of ACTFEL devices. The aging characteristics of a ZnS:Mn device are indicated in Fig. 6. The  $C$ - $V$  characteristics shift to higher voltages with respect to aging time. Note that this shift in the  $C$ - $V$  curves is an essentially rigid shift and is found to be

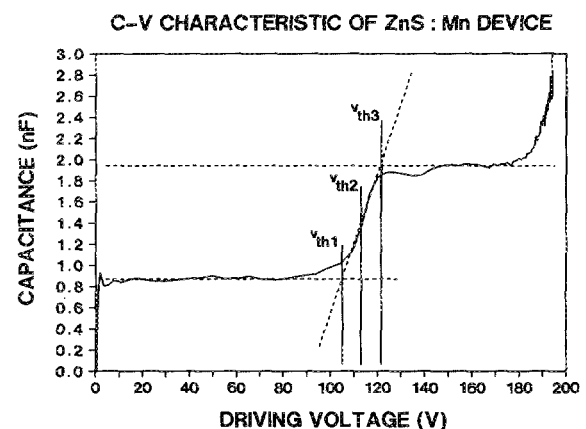


FIG. 5.  $C$ - $V$  curve for a ZnS:Mn ACTFEL device.

C-V CHARACTERISTICS AS A FUNCTION OF AGING  
ZnS:Mn DEVICE

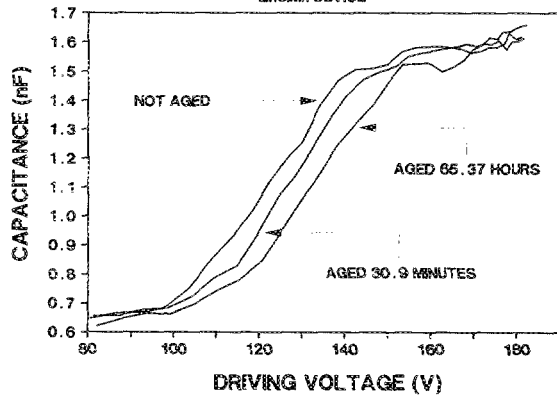


FIG. 6.  $C$ - $V$  curves as a function of aging time for a ZnS:Mn ACTFEL device.

logarithmic with respect to aging time. Although not evident from Fig. 6, it is found that the insulator and total capaci-

tances are independent of aging time, except near  $V_m$ .

In summary, we propose the  $C$ - $V$  technique as a means of exploring the electrical properties of ACTFEL display devices and we demonstrate the utility of the technique from an analysis of the  $C$ - $V$  and aging characteristics of a ZnS:Mn device. Although the  $C$ - $V$  technique may be regarded as an extension of the  $Q$ - $V$  technique, we believe  $C$ - $V$  analysis to be more readily interpretable in terms of the physics of the ACTFEL device.

This work was supported in part by the Air Force Office of Scientific Research under contract No. AFOSR 89-0309.

<sup>1</sup>Y. S. Chen and D. C. Krupka, *J. Appl. Phys.* **43**, 4089 (1972).

<sup>2</sup>D. H. Smith, *J. Lumin.* **23**, 209 (1981).

<sup>3</sup>K. W. Yang, S. J. T. Owen, and D. H. Smith, *IEEE Trans. Electron Devices* **ED-28**, 703 (1981).

<sup>4</sup>K. W. Yang, Ph.D. thesis, Oregon State University, 1981.

<sup>5</sup>R. Mach and G. O. Müller, *Phys. Status Solidi A* **69**, 11 (1982).

<sup>6</sup>P. M. Alt, *Proc. SID* **25**, 123 (1984).

<sup>7</sup>Y. A. Ono, H. Kawakami, M. Fuyama, and K. Onisawa, *Jpn. J. Appl. Phys.* **26**, 1482 (1987).

<sup>8</sup>E. Bringuier, *J. Appl. Phys.* **66**, 1316 (1989).